Multiport Investigation of the Coupling of High-Impedance Probes*

P. Kabos, *Senior Member IEEE*, U. Arz, *Member IEEE, and* D. F. Williams, *IEEE Fellow*

***Abstract*-- We used an on-wafer measurement technique that combines two- and three-port frequency-domain mismatch corrections in order to characterize the influence of a high-impedance probe on a device under test. The procedure quantifies the probe's load of the circuit, and the coupling between the probe and the device.**

***Index Terms*— high-impedance probes, invasiveness, three-port measurements**

I. Introduction

THE increased integration and operational speed of electronic circuits require a new approach to on-wafer metrology. Measurements at internal nodes of the integrated circuits or imaging of the circuit voltage/current maps with active and passive probes are becoming an important part of this new approach. We have recently developed a calibration technique for passive high-impedance probe (HIP) characterization [1] and [2].

Here we attempt to address one of the most complicated problems of probing metrology, namely the characterization of the influence of the probe coupling on the measured device under test (DUT) including the perturbation of the measured circuit performance due to the physical presence of the probe and the coupling to the neighboring active structures. We chose a simple geometry with the high-impedance probe introduced in different locations of the device. We used a combination of the previously developed two-port and multi-port procedures [3], [4] together with the high-impedance probe characterization described in [1].

II. Test Structure

Figure 1 shows an illustration of the experimental setup used in this study. The devices under test consisted of microstrip access lines with ground pads connected to the ground plane through via holes and a set of coupled lines terminated by different types of resistive and reactive loads. The length of the access lines was 250 μm, and the position of the on-wafer calibration reference planes for the device characterization coincided with the dashed line in Fig. 1. The position of the high-impedance probe with respect to the DUT is also depicted in Fig. 1. In position (1) the probe is off to the side of the circuit and the influence is expected to be less intrusive. In position (2) the high-impedance probe crosses the device lines and we expect stronger influence on the DUT.

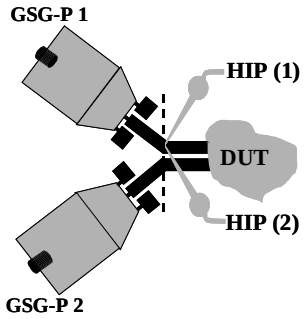

Figure 1 A sketch of the microstrip line artifacts used as devices in the experiment. The dashed line shows the position of the final on-wafer calibration reference plane. GSG–P1 and GSG-P2 are the ground-signal-ground probes. HIP (1), HIP (2) represent the position of the high-impedance probe in the two illustrated positions.

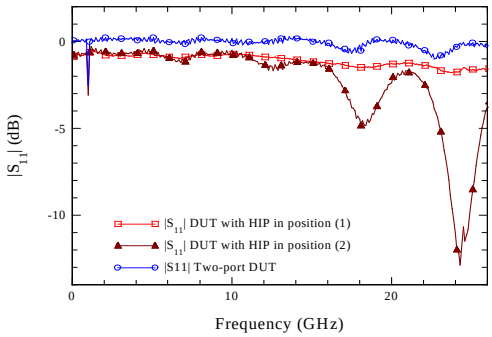

Figure 2 Magnitude of S_{11} for the open-ended coupled lines without the high-impedance probe (open circle symbols) and with the HIP in position (1) (open squares), and position (2) (solid triangles).

Figure 2 shows a measurement of $|S_{11}|$ as a function of frequency for open-ended coupled lines with the high-impedance probe (labeled "HIP" in the caption) in positions (1) (open square symbols) and (2) (solid triangles). Figure 2 also compares these measurements to $|S_{11}|$ in the absence of the high-impedance probe. The $|S_{11}|$ data in Fig. 2 are calibrated at the on-wafer reference planes after de-embedding the ground-signal-ground (GSG) probes. The procedures explained in [1] and [4] were implemented first. The data in Fig. 2 indicate a significant effect on the scattering parameters due to the high-impedance probe connected in position (2).

* Manuscript received XXXXX. P. Kabos and D. Williams are with the National Institute of Standards and Technology, Boulder, CO 80305 USA. U. Arz is with the Physikalisch-Technische Bundesanstalt in Braunschweig, Germany.

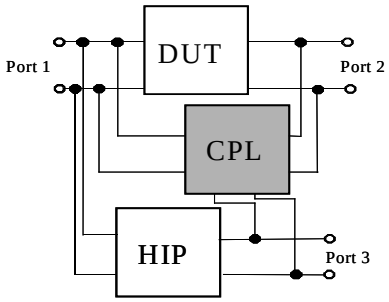

Figure 3 A model for the characterization of the HIP probe's influence on the measured DUT. The CPL three-port characterizes the additional influence of the probe, as described in the text.

III. Multi-port measurements

We used the four-port system described in [4]. The system consists of a conventional two-port vector network analyzer (VNA), and six computer-controlled broadband coaxial switches that connect the ports of the VNA to different probes. The switches are arranged so that the probes not connected to the ports of the VNA are terminated in nominally 50 Ω loads.

We began with a conventional first-tier four-port network-analyzer calibration at a set of coaxial reference planes, using the method described in [4]. This calibration accounts for imperfections in the measurement hardware, including its imperfect terminations. Next, we used this four-port calibration at the coaxial reference planes to characterize the three-port consisting of the GSG probes, the on-wafer DUT, and the high-impedance probe shown in Fig. 1.

However, our goal was not to characterize the GSG/DUT/high-impedance-probe combination at the coaxial reference planes, but rather to characterize the DUT and high-impedance-probe separately at the on-wafer reference planes shown by dashed lines in Fig. 1. To accomplish this, we determined the scattering parameters of the two GSG probes and the high-impedance probe in a separate two-tier calibration experiment. The first-tier calibration was at a coaxial reference plane and a second-tier calibration was done at an on-wafer reference plane in the microstrip lines. We established the on-wafer reference planes with a multiline Thru-Reflect-Line (TRL) calibration [5] with the reference impedance correction [6], [7]. The calibration artifacts are fabricated on alumina substrates. The structures include microstrip transmission lines 20.195 mm, 7.065 mm, 3.7 mm, and 2.635 mm long, a 0.5 mm long microstrip thru line, and a symmetric microstrip line reflect. From this two-tier calibration experiment we determined the two "error-boxes" corresponding to the scattering parameters of our two GSG probes.

We proceeded with measuring the 0.5 mm long microstrip line with a GSG probe at one port and the high-impedance probe on the other port. We then used the method described in [1] to de-embed the characteristics of the first GSG probe and the 0.5 mm microstrip line from the measurement. This procedure determines the scattering parameters of the high-impedance probe including the contributions from the 25-μm portion of the open-ended microstrip line, the parasitic capacitance of the open-ended microstrip line, and the high-impedance probe itself up to its coaxial connector.

Finally, we measured the DUT as a two-port device at the on-wafer reference planes. The first measurement was performed without the high-impedance probe whereas the following measurements include the high-impedance probe in positions (1) and (2) as a three-port device.

IV. Coupling and Invasiveness of the High-Impedance Probe

The above measurements provide the complete set of experimental data necessary to determine the influence of HIP. We proceed with comparing the three-port measurements with the combination of the two two-port HIP and the DUT scattering parameters. Any differences between the compared sets of data are due to the interaction between the high-impedance probe and the DUT. We introduced the circuit model shown in Fig. 3 in order to quantify this interaction. The notation of the matrices is defined in the figure caption. The additional three-port circuit labeled "CPL" represents the coupling of the high-impedance probe. We determined the "CPL" circuit from our three-port measurement of the DUT and high-impedance probe combination. To do this, we subtracted the two-port scattering parameters of the DUT and high-impedance probe from the measured three-port scattering parameters of the entire circuit by converting the measured scattering-parameter matrices to admittance parameters and converting the result, after the subtraction, back to scattering parameter matrix format.

The CPL scattering parameter matrix encompasses the contributions from both the coupling and the invasiveness (load) of the probe. We discuss both aspects separately below.

A. *Coupling*

Figure 4 shows, as an example, the calculated magnitudes of the S_{21}, S_{13}, and S_{32} scattering matrix coefficients for the high-impedance probe inserted in position (2). The coupling between ports 1 and 2, and ports 2 and 3 is negligible (on the order of – 20 dB over the whole frequency range).

This is not the case for the magnitude of the S_{13} parameter. The frequency response of $|S_{13}|$ shows a strong interaction between ports 1 and 3, surprisingly. Intuitively we would expect with the HIP in position (2) an increased coupling between ports 1 and 2. Instead, there is a strong additional signal at the output of the high-impedance probe produced by the crosstalk between the tip of the probe and the crossed line of the measured device.

A similar analysis for the high impedance probe in position (1) (not shown here) indicates that the coupling between ports 1 and 3 is in this case is also negligible. Here, the combination of the two-port scattering matrixes of the device and the high impedance probe is sufficient to characterize the system without invoking the CPL circuit.

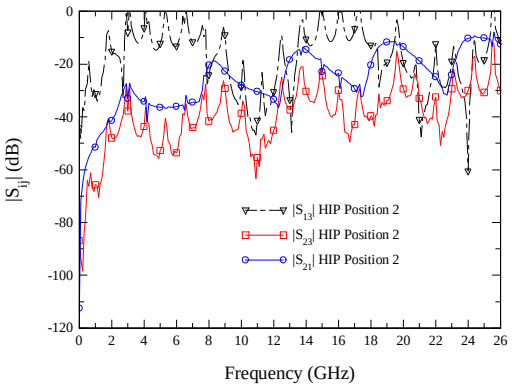

Figure 4 Magnitude of S_{12}, S_{13}, and S_{23} of the "CPL" coupling matrix elements in the presence of the HIP probe. The HIP probe is in position (2).

B. Load Impedance

In this section we examine the impedance the circuit is loaded with by the presence of the high-impedance probe. This load impedance can change the performance of the circuit and therefore plays an important role in practical applications.

There are several approaches for measuring the load (invasiveness) introduced by the probe to the device. Recently, we developed a procedure to quantify the invasiveness of the high-impedance probes with the aid of two-port measurements [8]. We also investigated, in detail, the repeatability and the relation of the load impedance to the measured parameters of the high-impedance probe.

Here, we use the three-port measurements to estimate the invasiveness in the presence of the coupling. The load impedance Z_{inv} is obtained from the reflection coefficient measured at one of the DUT ports with and without the high-impedance probe present. Figure 5 shows the magnitude of the impedance Z_{inv} as measured on the device consisting of open coupled-lines. There is an excellent agreement between the three-port measurements and the independent technique introduced in [8] for the high-impedance probe in position (1). In order to account for different microwave device structures, the impedance was corrected for the estimated fringe capacitance C_{fr} = 25 fF at the end of the microstrip line.

In reference [8] we showed that the load impedance of the high-impedance probe is closely related to the measured probe's scattering matrix parameters. Based on our three-port measurements we can further conclude that when the coupling is small (HIP in position (1)), the probe's characterization provides a good general estimate of the load impedance in the required frequency range. However, as follows from Fig. 5, when the coupling is stronger (HIP in position (2)), the estimate of the load impedance in such an environment is significantly compromised.

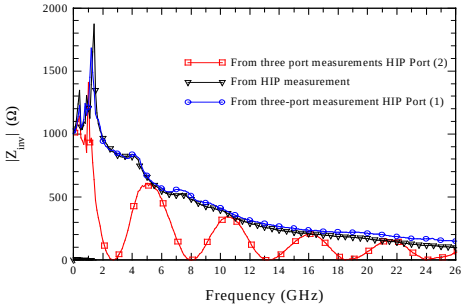

Figure 5 Magnitude of the load impedance. The line with open circle symbols represent the data obtained from three-port measurement for HIP in position (1), with square symbols from the three-port measurements for HIP in position (2), and with triangles represent data obtained from the high-impedance-probe characterization procedure.

V. Conclusions

We presented a study with intent to address the important problem of the influence of a probe on the properties of the measured device. We showed that simultaneous two- and three- port measurements provide reasonable information about the coupling. We demonstrated this on a commercially available high-impedance probe. We showed that the full two-port characterization of the high-impedance probe gives the required information about the probe's behavior. This information can prove to be useful in the development of coupling and invasiveness models for contact and non-contact high-frequency nanoscale metrology probes.

VI. Acknowledgement

The authors thank Dr. H.C. Reader for the match load calibration data used in the LRM calibration procedure and Dr. E. Gerecht for careful reading of the manuscript.

References

[1] U. Arz, H. C. Reader, P. Kabos, and D. F. Williams, "Wideband frequency-domain characterization of high-impedance probes," *58th ARFTG Conf. Digest, San Diego, CA, USA, Nov. 2001.*

[2] P. Kabos, H.C. Reader, U. Arz, and D. F. Williams, "Calibrated waveform measurement with high-impedance probes," *IEEE Trans. Microwave Theory Tech.*, 51(2): 530-535, Feb. 2003.

[3] R. F. Bauer and P. Penfield, "De-embedding and unterminating," *IEEE Trans. Microwave Theory Tech.*, 22(3): 282-288, March 1974.

[4] D. F. Williams, and D. K. Walker, "In-Line Multiport Calibration Algorithm," *51st ARFTG Conf. Digest*, pp. 88-90, June 12, 1998.

[5] R. B. Marks, "A multiline-method of network analyzer calibration," *IEEE Trans. Microwave Theory Tech.*, 39(7): 1205-1215, June 1991.

[6] R.B. Marks and D.F. Williams, "Characteristic Impedance Determination using Propagation Constant Measurement," *IEEE Microwave Guided Wave Lett.*, 1(6):141-143, June 1991.

[7] R.B. Marks and D.F. Williams, "A General Waveguide Circuit Theory," *J. Res. Natl. Inst. Stand. Technol.*, 97(5): 533-562, Sept.-Oct. 1992.

[8] U. Arz, P. Kabos, and D. F. Williams, "Invasiveness of high-impedance probes," *7th IEEE Workshop on Signal Propagation on Interconnects, Conf. Digest, Siena, Italy*, pp. 113-115., May 2003.